American Journal of Biochemistry and Biotechnology

Original Research Paper

Optimal Design of Dental Positioning Tracking Bracket for Oral Implant Surgery Navigation

[1]Lin Liu, [1,2]Miaosheng Guan, [1]Yiping Fan, [1]Hongchen Liu, [1]Hongbo Li and [3]Wenyu Niu

[1]Department of Stomatology, The First Medical Center of PLA General Hospital, No. 28, Fuxing Road, Beijing 100853, China
[2]PLA Rocket Force Characteristic Medical Center, No.16 Xinjiekou outside Street, Beijing 100088, China
[3]School of Computer Science and Artificial Intelligence, Wuhan University of Technology, Wuhan 430063, China

Article history
Received: 27-10-2022
Revised: 19-12-2022
Accepted: 27-12-2022

Corresponding Author:
Hongchen Liu
Department of Stomatology, The First Medical Center of PLA General Hospital, No. 28, Fuxing Road, Beijing 100853, China
Email: liu-hc301@hotmail.com

Abstract: The convergence of computer-aided technology and dental implant technology has shown that dynamic navigation technology can effectively improve the accuracy and reliability of clinical implant placement. To address this, a navigation system for oral implant surgery based on Mixed Reality (MR) technology has been developed. Using a standard dentition experimental model, the stability of linear and curved dental positioning and tracking brackets was studied by constructing a real-time monitoring system. The design and fixing methods of the positioning and tracking brackets were determined. The dental positioning and tracking bracket designed in this study provides a more accurate and convenient auxiliary implant bracket for implant surgery and ensures the accuracy of guided implant placement.

Keywords: Oral Implant Surgery, Surgical Navigation, Positioning and Tracking Bracket, Mixed Reality, Mechanical Analysis

Introduction

With the rise of oral implantology, the demands of doctors and patients for better treatment results are increasingly demanding. How to achieve the precise positioning of treatments has always been an important issue. Computer-assisted surgery has been used in neurosurgery since the end of the 19th century. The surgical guide is one of the effective methods to improve implant accuracy in clinical application: After Computerized Tomography (CT) scanning, the three-dimensional reconstruction information of the patient is obtained to place the implant in the ideal position through the computer system (Chen *et al*., 2021) different types of surgical guides are designed according to the implant positions designed by doctors. Although the implant-guided method can help clinicians to obtain ideal implant precision and its application also has limitations. For example, because the implant guide occupies a certain space when used in the mouth of some patients with limited openings, the intra-oral space cannot meet the requirements of implant treatment (El Kholy *et al*., 2019). This problem is more prominent in molar and other tooth positions. In addition, the gingiva and other soft tissues on the surface of the jaw will also affect the placement of the surgical guide, making it difficult to change the direction and depth of the implant after the guide is in place. Thus we try to build a navigation system (Wei *et al*., 2021; Aydemir and Arısan, 2020; Chen, 2019) that can dynamically guide high-precision planting without the aid of a static navigation device such as a surgical guide.

In the 1990s, Carolyn Heilbrun first proposed the navigation system device based on optical instruments. Currently, the optical navigation system has been widely concerned and used in dental and craniomaxillofacial surgery, such as temporomandibular joint surgery and oral implant. In our research, a Mixed Reality (MR) surgical navigation system is built to achieve high-precision implants assisted by optical navigation (Lungu *et al*., 2021; Joda *et al*., 2019; Viglialoro *et al*., 2021). In the three important components of the MR navigation system, the communication between the MR eyepiece and the NDI (Northern Digital Inc.) optical locator is a network system built through the wireless LAN, which is completed with the aid of computer algorithms. NDI optical positioning system mainly consists of an optical locator (a sensor capable of transmitting and receiving infrared light signals) and multiple-target tracking devices (each containing multiple sources that can generate or reflect signals). The navigation system mainly includes the following steps: (1) A tracking device agreed upon as a local coordinate system is fixed near the operation area of the patient; (2) The registration of the tracking device with the patient's surface markers is completed. This step needs to be realized by a computer algorithm, which has a great impact on surgical accuracy,

including point registration, surface registration, and mixed registration. Registration is a key operation in image-guided intervention, if the operation is improper, the results of the entire surgery may be affected; (3) The anatomical position of the patient is collected by the optical locator and mapped to the navigation software through the spatial position measurement and coordinate transformation; (4) The surgery is completed by computer navigation.

The Optical Tracking System (OTS) uses the light in the spectrum to monitor the attitude of the target object (Panchal *et al*., 2019; Stefanelli *et al*., 2019; Ma *et al*., 2019; Zhou *et al*., 2021). They are characterized by high tracking accuracy and sensitivity to environmental conditions and the main limitation is the requirement for a direct line of sight between optical markers and trackers. In the optical tracking system, the surgeon analyzes the position relationship between the surgical instrument and the patient's image data through the tracking system. Because the optical positioning devices have different recognition strategies for target markers, the optical positioning, and tracking system is divided into a "passive tracking system" and an "active tracking system". The active tracking system realizes positioning and tracking through the active luminous source equipped with the target marker and the passive tracking system is used to achieve target marker positioning and tracking through optical reflection (Bi *et al*., 2022; Alterman *et al*., 2019). Electromagnetic Tracking System (EMTS) uses an electromagnetic field to provide fast and accurate tracking without being limited by line of sight. Its main disadvantage is that it is prone to be distorted by nearby metal or ferromagnetic sources reducing the reliability of oral implant surgery navigation.

In recent years, virtual technologies such as Augmented Reality (AR) enable operators to observe the information on the original two-dimensional screen by wearing specific glasses (Huang *et al*., 2018; Pellegrino *et al*., 2019). It allows surgeons to visualize the 3D section information, 3D reconstruction image, or navigation information of the patient's jaw in real-time. However, there are few reports on the application of related technologies in stomatology, especially in oral implant, and research on clinical practice are rare. To improve the reliability of oral implant surgery navigation, we will study an oral implant navigation system based on MR technology (Mane *et al*., 2022; Frost *et al*., 2020; Pelanis *et al*., 2020). To realize the application of an optical positioning system in MR-guided oral implant, the optical passive tracking system is applied, that is, through the optical positioning ball, MR space registration two-dimensional code, and surgical tool tracking reference frame system to realize the connection of the computer, MR eyepiece, and patient anatomical site.

Design of Dentition Tracking Stent

A dentition tracking stent consists of three parts: The optical positioning ball end, the stent rod, and the dentition fixed base. As shown in Fig. 1, the base fixes the dental positioning tracking stent on the dentition through silicone rubber impression material:

(1) Design of optical positioning ball end: The optical set-ball layout used in this study is a cross-tracking head design recommended by Northern Digital Inc. of Canada. The four vertices of the cross are respectively equipped with NDI optical positioning balls, which can effectively detect the target position through the NDI system and successfully build a three-dimensional space system
(2) Design of dentition fixed base: The width of the base retention device is 1, 1.5, 2, 2.5, 3, 3.5, and 4 cm respectively (Fig. 1)
(3) Design of the stent rod: Referring to the existing dynamic implant navigation and the tracking stent length of the implant robot, the length of the stent rod is determined as 10 cm

Shape: It is designed as a linear and curved positioning tracking bracket as shown in Fig. 1.

Materials and Methods

Modeling and Mechanical Analysis of Dental Tracking Bracket System

Design and Mechanical Analysis of Linear Bracket

(1) Experimental hypothesis

Figure 1 is a simplified mechanical diagram of the linear dental tracking bracket considered in the paper. To facilitate the simulation, the paper assumes that the photosensitive resin materials are uniformly distributed and isotropic. The bracket size is approximately measured by the three-dimensional model in stl format. The position of the tooth end is simplified as the constraint of the fixed end. The support level is simplified to a sectional area of $A = h \times b = 0.535 \times 0.501 = 0.268$ cm^2, a length of $l = 9.2$ cm, and a uniformly distributed gravity load of $q = 2.99 \times 10\text{-}3$ N/c. The simplified cross-tracking head, passive infrared reflective sphere, and the connecting piece between them are one particle. The gravity is $P = (5.84+9.5+1.788\ \text{g}) \times 0.0098\ \text{N/g} = 0.168$ N and the single bracket stress is $F1 = P/2 = 8.39 \times 10\text{-}2$ N.

(2) Strength calculation

It can be seen from Fig. 2 that $F_2 = 0.111\ N$ and $M_A = 0.898$ N·cm, the maximum bending stressσis at point *A*. The calculation formula is as follows:

$$\sigma_A = \frac{M_{\max}}{W} = \frac{6M_A}{bh^2} = 0.376\text{MPa} \quad (1)$$

(3) Deflection calculation

It can be seen from Fig. 1 that the maximum angle (the included angle between the deformed bracket cross-section and the original cross-section) θ, the maximum deflection (the displacement of the centroid of the bracket cross-section in the direction of the vertical axis) w is all at point B. The calculation formula isas follows:

$$\theta_B = \int_0^l \frac{M}{EI}dx = \left[\frac{F_1 x}{EI}\left(\frac{l}{2} - x\right) + \frac{qx}{2EI}\left(lx - l^2 - \frac{x^2}{3}\right)\right] \Big|_0^l = -\frac{3F_1 l^2 + ql^3}{6EI} = -2.80 \times 10^{-3}\text{rad} \quad (2)$$

$$w_B = \int_0^l \left(\int \frac{M}{EI}dx\right)dx = \left[\frac{F_1 x^2}{6EI}(x - 3l) + \frac{qx^2}{24EI}(4lx - x^2 - 6l^2)\right] \Big|_0^l = -\frac{8F_1 l^3 + 3ql^4}{24EI} = -0.174\text{mm} \quad (3)$$

Design and Mechanical Analysis of Curved Bracket

(1) Experimental hypothesis

Figure 3 is a simplified mechanical diagram of the curved dental tracking bracket considered in the paper. To facilitate the simulation, the paper assumes that the photosensitive resin materials are uniformly distributed and isotropic. The bracket size is approximately measured by the three-dimensional model in stl format. The small segment of the bracket adjacent to the teeth end has double deformation of bending and torsion. However, the smaller size makes this segment of the bracket have good bending and torsion resistance and the mechanical analysis of this segment is ignored. The bracket is simplified as the bending beam with a sectional area of $A = h \times b = 0.4 \times 0.6 = 0.24$ cm^2, a uniformly distributed gravity load of $q = 2.68 \times 10^{-3}$ N/cm, the length of section $ABl_1 = 2.415$ cm, the length of section $BCl_2 = 3.365$ cm and $\angle ABC = 120°$. The simplified cross-tracking head, passive infrared reflective sphere, and the connecting piece between them are one particle and the gravity is P = (7.63+9.5 +1.788 g) × 0.0098 N/g = 0.185 N.

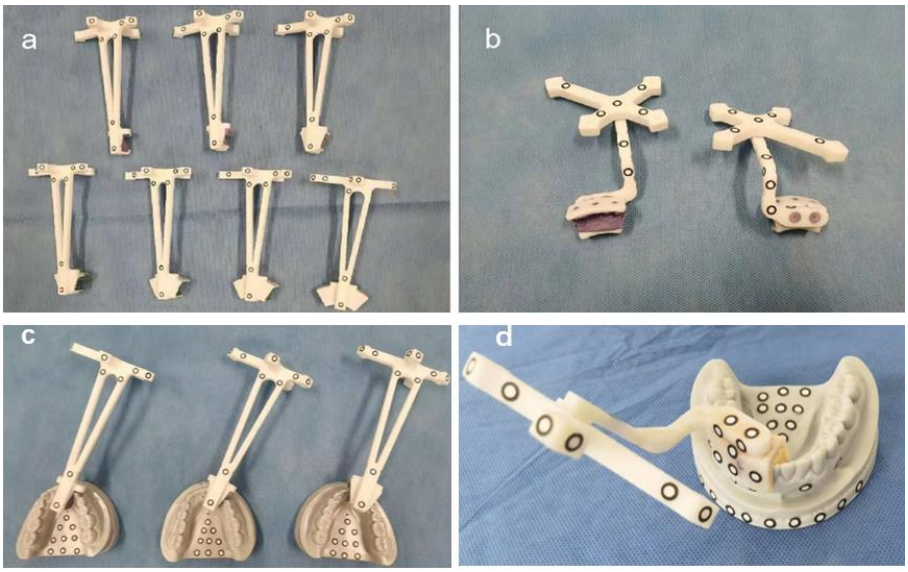

Fig. 1: Design of different specifications of dental tracking bracket

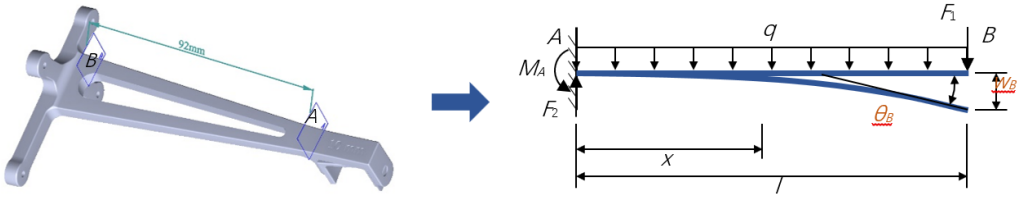

Fig. 2: Mechanical diagram of the linear bracket

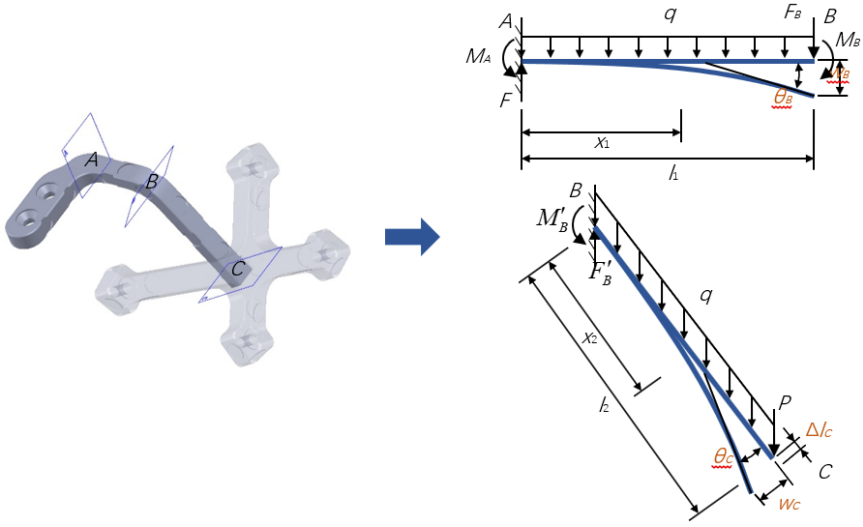

Fig. 3: Mechanical diagram of the bending bracket

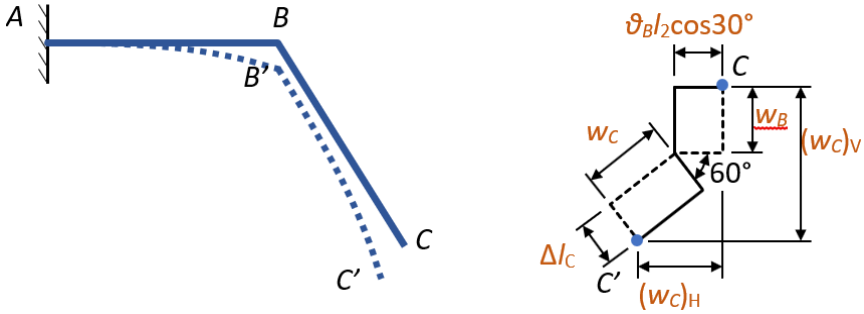

Fig. 4: Schematic diagram of the position change of point *C* of the curved bracket

(2) Strength calculation

As shown in Fig. 3, F = 0.201 N, M_A = 0.803 N·cm, F_B = 0.194 N, and M_B = -0.319 N·cm, the maximum bending stress$\sigma$is at point *A*. The calculation formula is as follows:

$$\sigma_A = \frac{M_{\max}}{W} = \frac{6M_A}{bh^2} = 0.502\text{MPa} \tag{4}$$

(3) Deflection calculation

It can be seen from Fig. 3 that the maximum angle θ and the maximum displacement w are at point *C*. The calculation formula is as follows:

$$\theta_B = \left[\frac{F_B x}{EI}\left(\frac{l_1}{2} - x\right) + \frac{qx}{2EI}\left(l_1 x - l_1^2 - \frac{x^2}{3}\right) - \frac{M_B x}{EI}\right]$$
$$\Big|_0^{l_1} = -\frac{3F_B l_1^2 + ql_1^3 + M_B l_1}{6EI} = -9.95\times10^{-5}\text{rad} \tag{5}$$

$$w_B = \left[\frac{F_B x^2}{6EI}(x - 3l_1) + \frac{qx^2}{24EI}(4l_1 x - x^2 - 6l_1^2) - \frac{M_B x^2}{2EI}\right]$$
$$\Big|_0^{l_1} = -\frac{8F_B l_1^3 + 3ql_1^4 + 12M_B l_1^2}{24EI} = -2.63\times10^{-2}\text{mm} \tag{6}$$

$$\theta_C = \left[\frac{Px}{EI}\left(\frac{l_2}{2} - x\right) + \frac{qx}{2EI}\left(l_2 x - l_2^2 - \frac{x^2}{3}\right)\right]$$
$$\Big|_0^{l_2}\cos 60° = -\frac{3Pl_2^2 + ql_2^3}{6EI}\cos 60° = -7.56\times10^{-4}\text{rad} \tag{7}$$

$$w_C = \left[\frac{Px^2\cos 60°}{6EI}(x - 3l_2) + \frac{qx^2\cos 60°}{24EI}(4l_2 x - x^2 - 6l_2^2)\right]$$
$$\Big|_0^{l_2} = -\frac{8Pl_2^3 + 3ql_2^4}{24EI}\cos 60° = -1.70\times10^{-2}\text{mm} \tag{8}$$

$$\Delta l_C = \left[\int_0^{l_2}\frac{q(l_2 - x_2)}{EA}\mathrm{d}x_2 + \frac{Pl_2}{EA}\right]$$
$$\sin 30° = \left(\frac{ql_2^2}{2EA} + \frac{Pl_2}{EA}\right)\cos 30° = 1.05\times10^{-4}\text{mm} \tag{9}$$

It can be seen that the position change of point *C* is affected by the superposition of the deformation of beams *AB* and *BC*, as shown in Fig. 4. The rotation angle of point *C*, horizontal displacement $(w_C)_H$, and vertical displacement $(w_C)_V$ are calculated as follows:

$$\theta'_C = \theta_B + \theta_C = 8.56\times10^{-4}\,\text{rad} \tag{10}$$

$$\begin{aligned}&(w_C)_H = -\theta_B l_2 \cos 30° - \sqrt{w_C^2 + \Delta l_C^2}\\ &\sin\left(arctan\frac{w_C}{\Delta l_C} - 30°\right) = -1.50\times10^{-2}\,\text{mm}\end{aligned} \tag{11}$$

$$\begin{aligned}&(w_C)_V = -w_B - \sqrt{w_C^2 + \Delta l_C^2}\\ &\cos\left(arctan\frac{w_C}{\Delta l_C} - 30°\right) = -4.10\times10^{-2}\,\text{mm}\end{aligned} \tag{12}$$

Experimental Results and Analysis

Theoretical Mechanical Analysis Results of the Bracket Structure

To solve the problem that the strength and structure of dental tracking brackets are difficult to be represented concretely in the actual medical applications, the solving ideas and theoretical research process of material mechanics and theoretical mechanics are introduced. First, according to the three-dimensional model and actual stress state of the linear bracket and personalized bending bracket, many assumptions are made to meet the needs of research and calculation. At the same time, the actual object is abstracted into a mechanical sketch that only retains the basic structure and explanatory symbols. Then the shear force and bending moment equations and integral method are used to calculate the structure in sections. Finally, the actual angle and deflection at the end of the bracket (far from the teeth) can be calculated by linear superposition of each angle and deflection. In the mechanical calculation of the bracket based on the basic mechanical knowledge, compared with the original bracket, the bending resistance and bearing capacity of the bracket after multiple simplified treatments decreases, and the calculated maximum bending stress, rotation angle, and deflection increase. Figures 2 and 3, compared with the original bracket, the bending resistance and bearing capacity of the bracket after multiple simplified treatment decrease, and the calculated maximum bending stress, rotation angle, and deflection increase. However, the calculated maximum bending stress is still only about 3‰ of the bending strength of the photosensitive resin material. The maximum rotation angle θ_B and the maximum deflection (displacement) w_B are small enough. Therefore, the strength and stiffness of the linear bracket meet the requirements and the self-weight of the bracket has little influence on the accuracy of the optical scanning calibration system.

Construction of a Real-Time Monitoring System

Figures 5 and 6, combining a high-precision scanning instrument with the vibration mode of the bracket system, an effective tool that can effectively monitor, track, shoot and analyze the displacement of the system in real-time is established. The system has good stability and the scanner registration error is about 0.005 mm, meeting the application requirements.

Specifically, the real-time monitoring system in Fig. 5 is mainly composed of four modules: (1) Aerospace optical grating scanner that is responsible for scanning and data acquisition. The main part of the scanner equipment is the probe, which is installed on a stable and reliable triangular support to ensure that the overall scanner is in a stable state during the subsequent scanning process to avoid scanning errors caused by shaking and other problems; (2) The dynamic motion device, with the NMYC-200 C horizontal decolorization shaker as the main part, is mainly responsible for simulating the dynamic surgical environment and the interference factors generated by the simulated motion state on the stability of the tracking system to simulate the clinical operation; (3) Experimental model part, this is the object to be observed in the experiment, that is, the dental positioning and tracking bracket; (4) The computer terminal is loaded with the aerospace optical grating scanning system software TriScan, which is responsible for collecting the relevant position information of the experimental model at a certain frequency.

To study the influence of different retention materials on the stability of the dental positioning and tracking bracket, the positioning and tracking bracket is first fixed at the arc corner of the maxillary and mandibular model dental arch. According to the retention materials, they are divided into three groups. The retention materials are 3 m Express XT hydrophilic addition silicone rubber, 3 m polyether fine impression material, and polycondensation silicone rubber. Then the real-time monitoring system is turned on with a detection frequency of 0 s/time and a detection time of 2 h. The horizontal shaker (frequency is 20 Revolutions Per Minute (RPM)) is used to simulate the shaking of the patient's maxillofacial area during implant navigation surgery. After 2 h of real-time monitoring, the tracking device is removed and replaced to complete the experiment.

Stability Analysis of Dental Positioning and Tracking Bracket

The in-depth experimental research on three different material bracket systems: Polycondensation Silicone Rubber (PSR), Addition Silicone Rubber (ASR), and Polyether Material (PM) are carried out respectively. The data results show that the bracket systems made of different materials have different stability significantly and the specific results are shown in Fig. 7.

According to the experimental results, it can be found that the tracking system will generally have a short-term excessive deformation at the beginning of bonding, resulting in a relative displacement between the bracket identification point and the model identification point, which is reflected in the overall displacement of the bracket tracking system.

In the application of PSR, there is a large displacement error after the bracket system is installed. Compared with the other two materials, except that the 2.0 cm width group has no statistical difference with the polyether group, the other two materials in the PSR group have the largest mean error as well as statistical differences with the other two materials, especially the 1.0 cm width bracket with a large error. In the ASR group, more stable relative displacement maintains between 0 and 0.2 mm and the 1.0-2.5 cm wide brackets also have the minimum relative displacement error. In the PM group, it can be seen that the racking system is also relatively stable and the bracket with a width of 3.0-3.5 cm shows the smallest relative displacement error.

Error Analysis of the Dentition Fixed Width and Material to the Dental Positioning and Tracking Bracket

Figure 8, through further analysis of different bracket widths in each experimental group, it is found that in the PSR group, 1.0, 1.5, 3.5, and 4.0 cm widths have a greater relative displacement of the bracket. The brackets with different widths of the polyether group can maintain relative stability and the addition of silicone rubber is the most stable. Between the relative error displacement of 0 and 0.15 mm, it can be seen from the broken line chart that the three materials with a width of 2.0-3.0 cm can maintain a low error displacement, which is about 0.05 mm.

The Influence of Bracket Rod Shape on the Stability

In the bending bracket system, both the system and the linear system are relatively stable and their stability performance has no significant change compared with the linear bracket system, as shown in Table 1.

Table 1: Stability analysis of bracket rod shape

	N	Mean	SD	P
Linear bracket	144	0.033	0.011	0.423
Personalized bracket	144	0.034	0.013	

Fig. 5: Measurement points of the real-time monitoring system of the system bracket

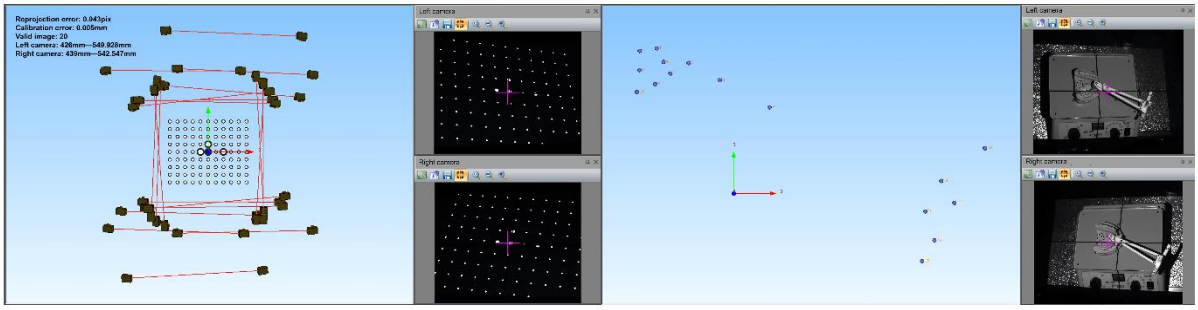

Fig. 6: Real-time monitoring device registration and experimental data acquisition interface

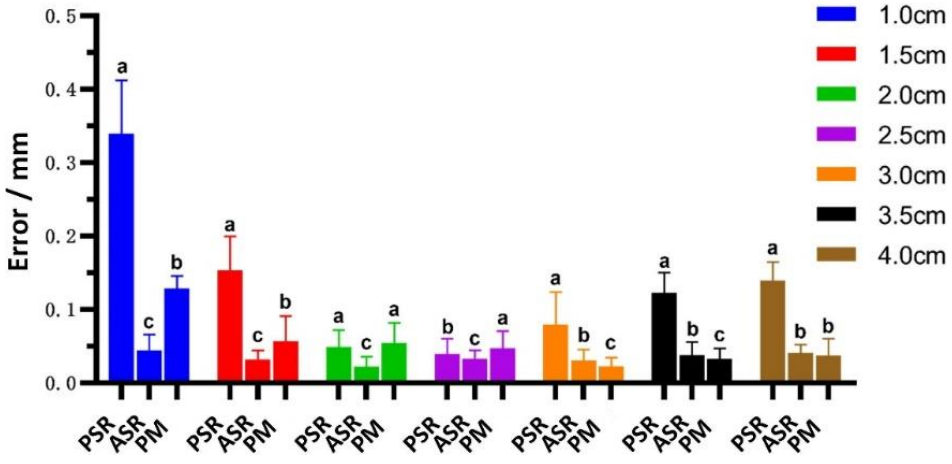

Fig. 7: Error analysis of bracket stability material factors

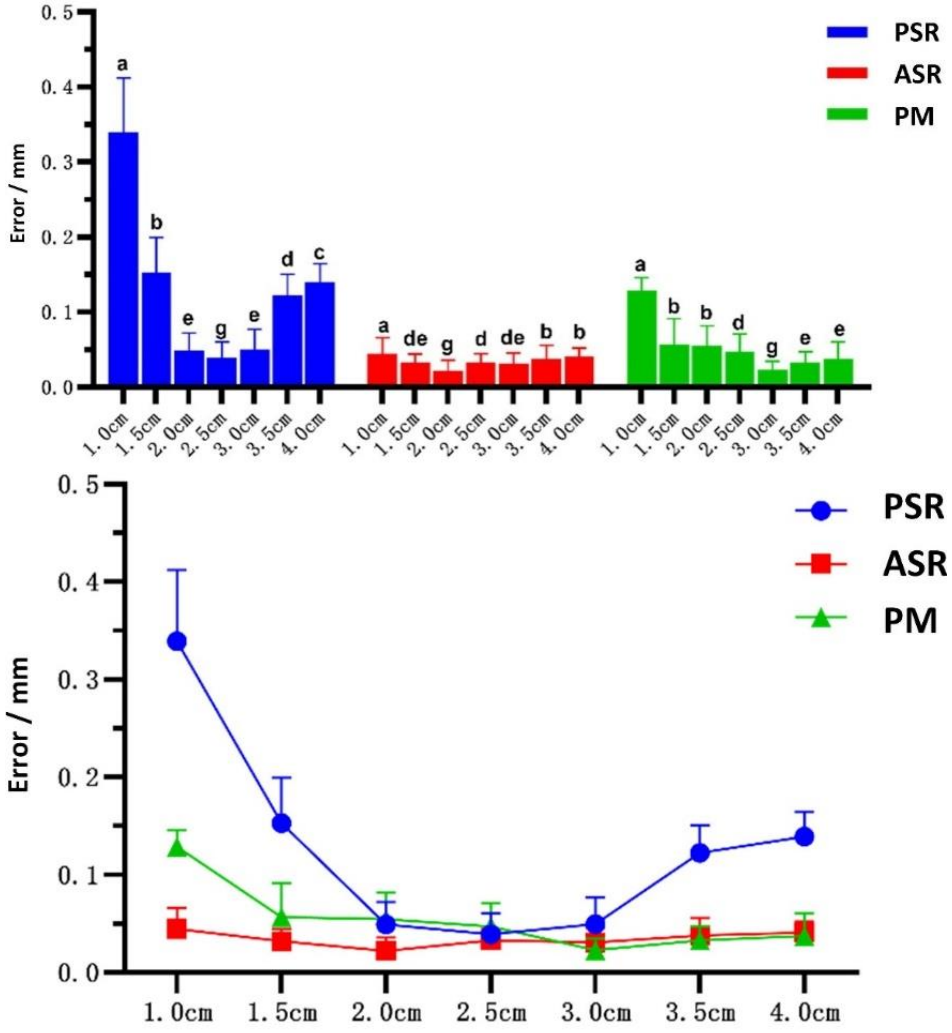

Fig. 8: Width error analysis of the bracket stability

Discussion

Factors Affecting the Instability of Dental Positioning and Tracking Bracket

Through the analysis and calculation of mechanical properties, it is proved that the strength and stiffness of the bracket meet the requirements and the stability and reliability of the bracket under dynamic scenarios are checked. In this experiment, a dynamic monitoring system is built with high-precision optical instruments to analyze the influence of different time points, retention widths of different bracket positioning and tracking systems, and different retention materials on the application of bracket positioning and tracking systems. During the experiment, different conditions and environments are set to simulate the clinical application environment. The landmark of the system and the landmark in the dental model are mainly used to reflect the relative displacement between the bracket and the dentition. At the same time, a dynamic monitoring system is added, that is, the dental movement device simulates the influence of posture change of patients on the dynamic monitoring in clinical application. Generally, except for the obvious displacement in the PSR group, the other groups remained relatively stable despite the displacement.

In addition, different retentive widths are designed for different retentive capabilities of brackets, including seven groups of gradient experimental widths from 1.0 to 4.0 cm. The experiment found that different from the greater the retentive width, the better the retention effect, in theory, the brackets with a width of 1.0 and 4.0 cm in PSR have a large displacement at the beginning. In the case of excluding systematic errors, when the retentive width is small, the retentive capacity of the bracket is insufficient, which may cause instability of the bracket in motion. The wider the width, the worse the restoration of the base brackets. In addition, in clinical practice, because of the tooth position where the bracket can be placed, it is considered that the front teeth of the premolars are in place, simulating the arch of the dentition due to the opening tension and mouth angle. Wider brackets are more prone to friction contact with labial muscles and dentition, resulting in problems such as the fulcrum at the bottom of the base bracket cannot be fully placed and uneven thickness of retention materials, which ultimately leads to instability of the system. Thus it is not suitable for the width of the bracket tracking device to be too short and too wide and it can maintain a relatively stable stent state in 2.0-3.0 cm.

Concerning different retention materials, i.e., PSR, ASR, and PM were used as three retention materials for experiments. The results showed that the early stability of PSR was worse than that of the other two groups and the ASR group and PM group were relatively stable. Considering that the deformation of the retention material changes the stability of the time-point detection bracket, the retention material of the bracket is deformed at the initial stage and an unstable state at the later stage, we believe that the short-term change of the bracket mainly comes from the deformation caused by the elasticity of the retention material rather than the plastic deformation.

Factors that Affect the Stability and Deformation of the Dental Tracking Bracket Fixed in the Dentition, the Following Head and Mandibular Movement

Ideally, the spatial position of patients marked by the bracket system does not change. In practice, the posture adjustment of patients, the change of the bracket, and the difference between the impression materials used for bracket retention are all factors that affect implant precision.

The dental implant surgery is performed under local anesthesia. During the operation, only the affected part is anesthetized and the patient remains conscious all the time. The advantage is that in the surgery, the degree of communication and postural coordination is better. The disadvantage is that during the whole surgical process, the patient can feel some tension or psychological burden and cannot keep static, causing some conscious or unconscious actions. This requires that the tracking device has good stability to be recognized and cooperates with the NDI system to achieve effective target positioning. (1) Changes in patient posture: In the process of clinical dental implantation, the patient is under local anesthesia and will have a certain degree of mobility in the treatment, which is a certain degree of change. Moreover, due to the needs of the clinical operation, the doctor needs to change the position of patients to obtain a good surgical vision, which requires the positioning and tracking bracket to have good recognition ability and cooperate with the NDI system to achieve effective positioning of the target. (2) One end of the intraoral tracking system is fixed to the dentition of patients through adhesive materials and the other end is a tracking and positioning system. Both ends are connected through the rod. The too-long rod is easy to cause one end of the tracking system to shake and the rod is easy to cause the identification of the occlusion tracking system during operation. According to relevant literature and the existing commercial planting navigation/robot bracket design forms, we combine the length of a commercial fixed tracking rod with the maximum linear measurement distance of about 10cm as the limit length. Thus in the experiment, the length of the designed tracking and positioning rod is 10cm to measure the maximum value. (3) The tracking bracket mainly involves the stability of the retention material and the size of the retention force provided by the retention device. The retention materials are mainly impression materials that are widely used in the clinic, such as silicone rubber impression materials, polyether impression materials, and more. The retention force, to a large extent, relates to the structural areas such as the contact undercut between the

retention base and the tooth position, which can effectively improve the stability of the tracking stent. (4) Patient mouth opening: In clinical application, the tracking system is mainly placed in the median and lateral position, the premolar area of the oral corner. If the positioning and tracking bracket is fixed near the posterior tooth area, it is easy to be pulled by the muscle of the mouth corner to cause bracket loosening. If the tracking bracket is fixed in the middle position, it may cause the operator to block the tracking system from capturing the position. It is thus necessary to design a tracking system with a personalized bent bracket structure for patients with small mouth openings.

In clinical application, the tracking system is mainly placed in the anterior area of the oral corner of the lateral incisors, canines, and dental arch. If the bracket is placed back, it is easy to shake or dislocate due to the interference of anatomical structures such as mouth opening degree and mouth angle. If the bracket is placed in the front, it may also interfere with the operating vision. To this end, after studying the stability of the bottom bracket width of the linear tracking bracket, the design appearance is improved into a personalized curved bracket and the tracking system with the best bottom bracket width.

Conclusion

This research is based on the navigation system of oral implant surgery with Mixed Reality technology (MR). Using the standard dentition experimental model, the stability of the personalized dentition positioning tracking stent system model is studied by constructing a real-time monitoring system and the design mode and fixing method of the positioning tracking stent are clarified. The experimental results show that the strength and stiffness of linear and curved dental tracking brackets meet the requirements and the best fixing width of the base is between 2.0 and 3.0 cm to maintain the stability of the bracket. The dental tracking bracket designed in this study can provide technical support for improving the reliability of oral implant surgery.

Author's Contributions

Lin Liu and Miaosheng Guan: Designed and performed the experiments, analyzed the data, and prepared the paper.

Yiping Fan, Hongchen Liu and Hongbo Li: Participated to collect the materials related to the experiment.

Wenyu Niu: Designed the experiments and revised the manuscript.

Funding Information

This study was supported by a grant from the Special Project on Health Care of China (No. 19BJZ18).

Data Availability Statement

The raw data supporting the conclusions of this article will be made available by the authors, without undue reservation.

Ethics

The authors declare their responsibility for any ethical issues that may arise after the publication of this manuscript.

Conflict of Interest

The authors declare that they have no competing interests. The corresponding author affirms that all of the authors have read and approved the manuscript.

References

Alterman, M., Rushinek, H., Lavi, A., & Casap, N. (2019). Computerized navigation for minimal invasive retrieval of displaced dental implants in the lower jaw. *Oral and Maxillofacial Surgery Clinics*, *31*(3), 447-455. https://doi.org/10.1016/j.coms.2019.03.007

Aydemir, C. A., & Arısan, V. (2020). Accuracy of dental implant placement via dynamic navigation or the freehand method: A split-mouth randomized controlled clinical trial. *Clinical Oral Implants Research*, *31*(3), 255-263. https://doi.org/10.1111/clr.13563

Bi, S., Wang, M., Zou, J., Gu, Y., Zhai, C., & Gong, M. (2022). Dental Implant Navigation System Based on Trinocular Stereo Vision. *Sensors*, *22*(7), 2571. https://doi.org/10.3390/s22072571

Chen, J. T. (2019). A novel application of dynamic navigation system in socket shield technique. *Journal of Oral Implantology*, *45*(5), 409-415. https://doi.org/10.1563/aaid-joi-D-19-00072

Chen, Y. W., Hanak, B. W., Yang, T. C., Wilson, T. A., Hsia, J. M., Walsh, H. E., Shih, H.C., Nagatomo, K. J. (2021). Computer-assisted surgery in medical and dental applications. *Expert Review of Medical Devices*, *18*(7), 669-696. https://doi.org/10.1080/17434440.2021.1886075

El Kholy, K., Lazarin, R., Janner, S. F., Faerber, K., Buser, R., & Buser, D. (2019). Influence of surgical guide support and implant site location on the accuracy of static Computer-Assisted Implant Surgery. *Clinical Oral Implants Research*, *30*(11), 1067-1075. https://doi.org/10.1111/clr.13520

Frost, J., Chipchase, L., Kecskes, Z., D'Cunha, N. M., & Fitzgerald, R. (2020). Research in brief: Exploring perceptions of needs for the same patient across disciplines using mixed reality: A pilot study. *Clinical Simulation in Nursing*, *43*, 21-25. https://doi.org/10.1016/j.ecns.2020.02.005

Huang, T. K., Yang, C. H., Hsieh, Y. H., Wang, J. C., & Hung, C. C. (2018). Augmented reality (AR) and virtual reality (VR) are applied in dentistry. *The Kaohsiung Journal of Medical Sciences*, *34*(4), 243-248. https://doi.org/10.1016/j.kjms.2018.01.009

Joda, T., Gallucci, G. O., Wismeijer, D., & Zitzmann, N. U. (2019). Augmented and virtual reality in dental medicine: A systematic review. *Computers in Biology and Medicine*, *108*, 93-100. https://doi.org/10.1016/j.compbiomed.2019.03.012

Lungu, A. J., Swinkels, W., Claesen, L., Tu, P., Egger, J., & Chen, X. (2021). A review on the applications of virtual reality augmented reality and mixed reality in surgical simulation: An extension to different kinds of surgery. *Expert Review of Medical Devices*, *18*(1), 47-62. https://doi.org/10.1080/17434440.2021.1860750

Ma, L., Jiang, W., Zhang, B., Qu, X., Ning, G., Zhang, X., & Liao, H. (2019). Augmented reality surgical navigation with accurate CBCT-patient registration for dental implant placement. *Medical & Biological Engineering & Computing*, *57*(1), 47-57. https://doi.org/10.1007/s11517-018-1861-9

Mane, T., Bayramova, A., Daniilidis, K., Mordohai, P., & Bernardis, E. (2022). Single-camera 3D head fitting for mixed reality clinical applications. *Computer Vision and Image Understanding*, *218*, 103384. https://doi.org/10.1016/j.cviu.2022.103384

Panchal, N., Mahmood, L., Retana, A., & Emery, R. (2019). Dynamic navigation for dental implant surgery. *Oral and Maxillofacial Surgery Clinics*, *31*(4), 539-547. https://doi.org/10.1016/j.coms.2019.08.001

Pelanis, E., Kumar, R. P., Aghayan, D. L., Palomar, R., Fretland, Å. A., Brun, H., Edwin, B. (2020). Use of mixed reality for an improved spatial understanding of liver anatomy. *Minimally Invasive Therapy & Allied Technologies*, *29*(3), 154-160. https://doi.org/10.1080/13645706.2019.1616558

Pellegrino, G., Mangano, C., Mangano, R., Ferri, A., Taraschi, V., & Marchetti, C. (2019). Augmented reality for dental implantology: A pilot clinical report of two cases. *BMC Oral Health*, *19*(1), 1-w8.

Stefanelli, L. V., DeGroot, B. S., Lipton, D. I., & Mandelaris, G. A. (2019). Accuracy of a Dynamic Dental Implant Navigation System in a Private Practice. *International Journal of Oral & Maxillofacial Implants*, *34*(1). 205-213.

Viglialoro, R. M., Condino, S., Turini, G., Carbone, M., Ferrari, V., & Gesi, M. (2021). Augmented reality, mixed reality and hybrid approach in healthcare simulation: A systematic review. *Applied Sciences*, *11*(5), 2338. https://doi.org/10.3390/app11052338

Wei, S. M., Zhu, Y., Wei, J. X., Zhang, C. N., Shi, J. Y., & Lai, H. C. (2021). Accuracy of dynamic navigation in implant surgery: A systematic review and meta-analysis. *Clinical Oral Implants Research*, *32*(4), 383-393. https://doi.org/10.1111/clr.13719

Zhou, M., Zhou, H., Li, S. Y., Zhu, Y. B., & Geng, Y. M. (2021). Comparison of the accuracy of dental implant placement using static and dynamic computer-assisted systems: An in vitro study. J*ournal of Stomatology, Oral and Maxillofacial Surgery*, *122*(4), 343-348. https://doi.org/10.1016/j.jormas.2020.11.008